

Ultrafast Synthesis and Coating of High-Quality β -NaYF₄:Yb³⁺,Ln³⁺ Short Nanorods

Fabrizio Guzzetta,[†] Anna Roig,^{*,‡} and Beatriz Julián-López^{*,†}

[†]Institute of Advanced Materials (INAM), Universitat Jaume I, Av. Sos Baynat s/n, 12071 Castellón, Spain

[‡]Institut de Ciència de Materials de Barcelona (ICMAB-CSIC), Campus de la UAB, 08193 Bellaterra, Spain

Supporting Information

ABSTRACT: An ultrafast route to prepare up-converting single β -phase NaYF₄:Yb³⁺,Ln³⁺ (Ln: Er, Tm, or Tb) short nanorods (UCNRs) of high quality was developed. This new procedure affords reactive-surface nanorods that are easily coated by direct injection of suitable capping ligands. Thus highly crystalline nanorods with excellent UC fluorescence and good solvent-selective dispersion are obtained, which represents a significant advance in the field and enlarges their use for biomedical and other technological applications. Unlike other methodologies, the short reaction time provides a kinetic control over crystallization processes, and the β -phase and rod morphology is preserved regardless of the optically active Ln³⁺ ion. The UC emission was finely tuned by using the most popular Yb³⁺/Tm³⁺ and Yb³⁺/Er³⁺ pairs. More importantly, UCNRs doped with the unusual Yb³⁺/Tb³⁺ pair, with no ladder-like energy levels, provided a nice emission upon near-infrared excitation, which constitutes the first example of phonon-assisted cooperative sensitization to date in pure β -NaYF₄ nanocrystals.

UC β -NaYF₄:Yb³⁺/Ln³⁺ Nanorods



Lanthanide-codoped β -NaYF₄ nanocrystals (Ln³⁺: Er, Tm, Yb) are high-brightness near-infrared (NIR) to visible-light up-converters with great interest in technological applications across many fields such as photonics, security, sensors, energy, and biomedicine.^{1,2} The key for their effective industrial integration in commercial devices will be the prospect to fabricate monodisperse high-quality nanocrystals with nanometric size (<100 nm), well-defined shape of pure hexagonal (β) phase, which affords the highest optical emission through a facile, cheap, and fast scalable synthetic route. Furthermore, a one-pot processing to make solvent-soluble dispersions of the nanoparticles is highly desirable.³

Up-converting nanoparticles (UCNPs) are routinely prepared by thermal decomposition,^{4–7} coprecipitation,^{8,9} and hydro- or solvothermal^{10,11} routes. However, harsh conditions such as high reaction temperature (>300 °C) and pressure, long reaction times (6–48 h), or waterless oxygen-free conditions are usually required, hindering their industrial up-scaling. Furthermore, NaYF₄ crystallizes first as a metastable cubic α -phase with very poor optical activity. The cubic-to-hexagonal conversion needs to overcome a high free-energy barrier,¹² and a subsequent fast growth of crystals occurs; thus mixtures of both phases are usually obtained, especially in the case of small nanoparticles.

Microwave-assisted (MW) synthesis has appeared as an attractive way to prepare monodisperse colloids with complex kinetic/thermodynamic control over crystallization processes.^{13,14} Indeed, this route has already been employed to prepare different fluoride materials.^{15–17} However, the accurate attribution of the crystalline phase is difficult in small nanocrystals and even sometimes avoided by the authors

because it is a crucial issue in highly sensitive luminescent systems. Reports concerning UC NaYF₄ encompass either small nanoparticles (<8 nm) of the 10-times less efficient α -phase^{18–20} and α/β mixtures²¹ or pure β -phase prisms^{20,22} and long wires²³ of micrometric size. Small nanorods of <100 nm, highly crystalline, and pure β -phase by using a mild and fast microwave route have never been reported to our knowledge.

An additional advantage of our MW protocol is that a functional coating can be added upon completion of the reaction.²⁴ This allows great versatility in designing stable colloids in solvents of different polarity in sight of the envisaged application. For example, in biologically relevant applications such as bioimaging, drug targeting, or nanothermometers, luminescent nanoparticles must be water-dispersible to be compatible under physiological conditions.²⁵ By contrast, other technological applications need their dispersion in low boiling solvents such as cyclohexane to make thin films in miniaturized designs. This is the case for solar cells, optoelectronic devices, or anticounterfeiting systems.^{26,27}

Here we present a fast, energy-efficient, and versatile microwave route to successfully prepare pure β -NaYF₄:Yb³⁺,Ln³⁺ nanorods (NRs) surface coated for solvent-selective dispersions. Along with the so-characterized Er³⁺ and Tm³⁺ ions as Ln³⁺ activators, we focused also on Tb³⁺ ions because it shows an unusual upconversion process. The distinctive energy level structure of Tb ions does not match with the 980 nm excitation. However, the long-lived excited ⁵D₄

Received: September 18, 2017

Accepted: November 10, 2017

Published: November 10, 2017

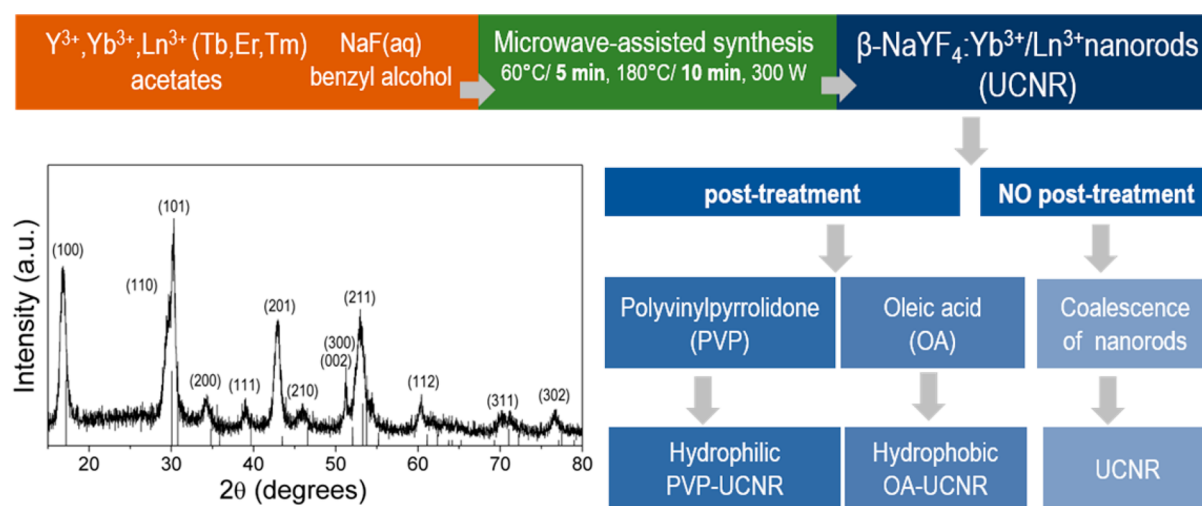


Figure 1. Schematic representation of the MW synthesis and post-treatment (PT) coating of the UCNR. XRD pattern of the β -NaYF₄:Yb,Tb³⁺ nanorods (β reference, JCPDS card 16-0334).

level can be populated based on the energy migration mechanism²⁸ in which two adjacent Yb³⁺ ions cooperatively sensitize one Tb³⁺ ion. This process has been demonstrated in Yb,Tb-codoped single crystals of SrCl₂²⁹ and ceramic glasses containing LiYbF₄,³⁰ NaLuF₄,³¹ and NaYF₄³² nanocrystals but very scarcely reported on NaGdF₄³³ and α -NaYF₄³⁴ nanoparticles. This approach can also be extended to other lanthanide ions such as Eu³⁺, Dy³⁺, or Sm³⁺ and afford tunable emissions spanning from the UV to the visible spectral region. Thus this simple and universal strategy to prepare NIR-activated fluorescent β -NaYF₄ nanorods represents a significant advance in the field.

Figure 1 summarizes the procedure to synthesize the up-converting nanorods; the details of the synthesis are included in the Supporting Information (SI). The precursors and solvent, F/Y ratio, and MW reaction conditions (T , t) have been judiciously modified to target nanometric dimensions and the single $P6_3/m$ hexagonal phase, as shown in the XRD pattern of Figure 1. The reaction conditions investigated to attain the pure β -phase are summarized in Table S11 and Figure S11. The optimized synthesis employs benzyl alcohol and lanthanide acetates as solvent and Ln³⁺ precursors, respectively.

Benzyl alcohol and benzyl mercaptan have previously been employed to prepare metal oxides³⁵ and sulfides³⁶ by nonaqueous routes with good results in controlling particle size but have never been tried for the synthesis of fluoride crystals. In such studies, the alcohol and mercaptan groups promoted the metal–oxygen–metal and metal–sulfur–metal bonds. The synthetic route reported here is not analogous because the main role of the benzyl alcohol is to act as a suitable solvent in terms of solubility in water (4 g/100 mL), thermal stability (boiling point of 205 °C), and probably as capping agent minimizing the nanocrystal aggregation. Although a detailed mechanistic study goes beyond the scope of this communication, the results will be shortly discussed.

The synthesis of the UC nanorods includes a preheating at 60 °C to completely dissolve the lanthanide acetates and the sodium fluoride in the benzyl alcohol/water mixture (4/1 molar ratio). The use of lanthanide acetates instead of stearates, which are salts commonly employed in the synthesis of lanthanide-doped fluoride nanocrystals,³⁷ favors the dissolution of the precursors without significant coordinating effect of the

acetate ligand. After 5 min at 60 °C, the temperature is rapidly increased to 180 °C and kept for 10 min. In this step, the kinetically controlled nucleation of α -NaYF₄ seeds and the nanocrystal growth promoting the α -to- β phase³⁸ transformation takes place. Further growth of the thermodynamically favored β -NaYF₄ phase is drastically reduced by a fast cooling of the reactor.

We further take advantage of the particles surface reactivity just after the MW synthesis to graft hydrophilic, such as polyvinylpyrrolidone (PVP), or hydrophobic, such as oleic acid (OA), molecules on the particle's surface. A functional coating was formed by simple injection of the capping ligands into the reaction tubes, which were kept at 80 °C after the nanocrystals synthesis to better preserve their surface reactivity. We adopted this strategy instead of the addition of PVP or OA during the UCNRs synthesis because both molecules were demonstrated to suffer oxidation or degradation processes during the microwave treatment. The formation of PVP- and OA-capped UCNRs was verified by FTIR analysis (Figure S12).^{39–41}

Figure 2a shows a TEM image of the bare UCNRs doped with Tb, as an example. The particles exhibit an anisotropic morphology with rather uniform transversal size (or diameter) of ~15 nm and a longitudinal size distribution ranging between 30 and 100 nm (Figure 2e). The rods appear stacked along the longitudinal axis, forming small aggregates of few NRs. In accordance to the XRD results, the diffraction rings of the SAED patterns for the UCNRs (Figure 2d) were indexed to the β -phase.

In comparison with previous reports in which MW routes are used to prepare small monodisperse α -NaYF₄ nanocrystals,¹⁸ our synthesis of β -NaYF₄ nanorods provides larger but less uniform particle sizes. The larger sizes are beneficial for the UC photoluminescence because it is well-established that the particle size dramatically influences the nonradiative properties (multiphonon relaxation and energy transfer), reducing the UC efficiency drastically from values of 13 to 14% to 0.001% in Er,Yb:NaYF₄ particles of a few microns to a few nanometers (<8 nm). This effect is related to the presence of defects at the surface of the nanocrystals.^{42,43} Regarding the less uniform morphology, we can find an explanation on the model of phase transition reported by Berry.³⁸ We hypothesize that the size polydispersity would be related to small differences in the

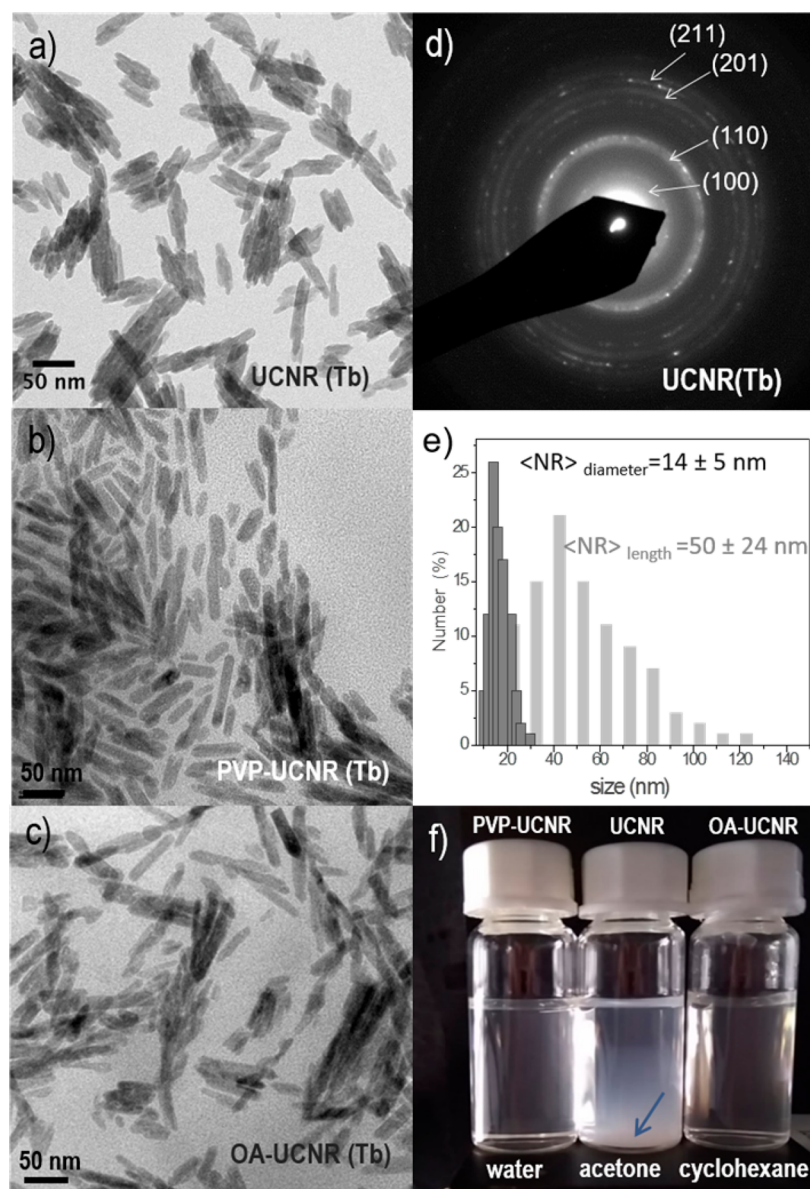


Figure 2. (a–c) TEM images of the bare, PVP-coated and OA-coated UCNRs, respectively. (d) SAED image from bare Tb-NRs. (e) Transversal and longitudinal size distribution of Tb-NRs. (f) Dispersion of the Tb-NRs in different solvents.

duration of the stage during which the α particle ripens, before β particles begin to appear. Therefore, it would be interesting to explore in the future if mild annealing conditions for a long time can be used to refine nanomaterials shape. Anyway, the described methodology provides pure hexagonal nanorods in extremely short time (15 min) with excellent up-conversion luminescence intensity.

After coating with PVP molecules (see Figure 2b), the small aggregates disappear and the nanorods are found isolated with an average inter-rods distance of ca. 8 nm, a distance compatible with a uniform PVP coating. In the case of OA-grafted NRs, the particles also appeared less aggregated than for the bare UCNr, but the inter-rod distance is not so evident (Figure 2c). Figure 2f depicts the nanoparticles stability in polar and nonpolar solvents. The as-obtained rods quickly sediment in all solvents (acetone is used here to illustrate this fact). In contrast, the rods coated with PVP are colloidal stable for months when dispersed in water; similarly, the particles coated with oleic acid remain well dispersed in cyclohexane.

Figure 3 shows that the hexagonal crystal phase and the rod-like morphology are maintained under the same reaction conditions independently of the emitting lanthanide ion employed (terbium, erbium, and thulium). This fact highlights the universal kinetic control of the crystal growth in this MW-assisted synthesis, allowing us freedom of choice of multilined emissions. The Figure also evidences the lanthanide-doping-mediated crystal growth process reported by Wang,⁴⁴ where the dimensions of the NRs are little affected by the ionic radius and dipole polarizability of the substitutional dopant ion (increasing ionic radius or polarizability $Tm < Er < Tb$).

The MW-synthesized $NaYF_4$ nanorods exhibited excellent up-conversion emission. Figure 4 shows the photographs of the three-doped systems emitting visible light (mainly green and blue light at naked eye) upon 980 nm excitation. The UC emission spectra of PVP-coated nanorods are illustrated in Figure 4, left. The optical analysis was done in water suspensions for convenience because the emissions of the crystalline nanorods are hardly affected by the coating. The

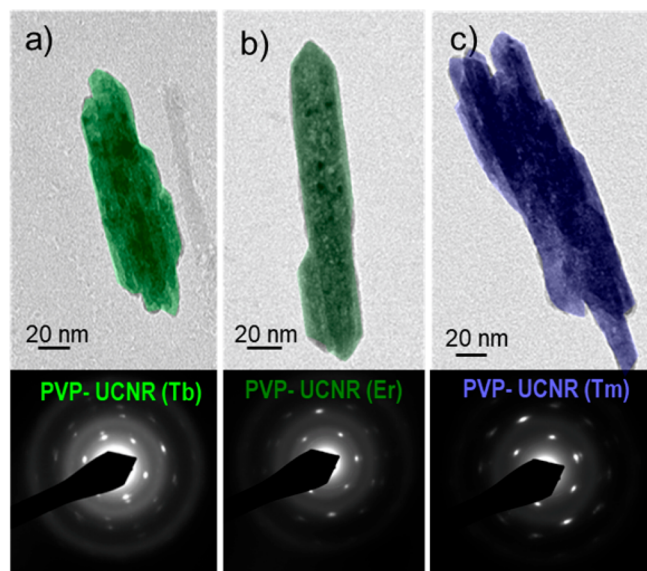


Figure 3. TEM images and SAED patterns of PVP-UCNRs doped with (a) Yb,Tb-, (b) Yb,Er-, and (c) Yb,Tm-NaYF₄ hexagonal nanorods.

spectra display the characteristic emission bands from the $f-f$ electronic transitions of Tb³⁺, Er³⁺, and Tm³⁺ ions ascribed in the spectra upon NIR irradiation. These transitions correspond to the well-established UC mechanism for Er/Yb (two-photon absorption) and Tm/Yb (three-photon absorption) doping pairs,⁴⁵ in which the efficient upconversion is associated with

their ladder-like arranged energy levels facilitating the successive photon absorption (Figure 4, right).

It is remarkable to see the intense manifold emissions from $^5D_4, ^5D_3 \rightarrow ^7F_J$ ($J = 6, 5, 4, 3$) transitions of Tb³⁺ generated by excitation of two Yb³⁺ ions and simultaneous energy transfer at the ground state 7F_6 , which then populates the excited 5D_4 and 5D_3 levels.³⁴ To our knowledge, this is the first example of phonon-assisted cooperative sensitization in pure β -NaYF₄:Yb³⁺,Tb³⁺ to date.

The visible color emission is efficiently tuned by changing the activator ion (Tm, Tb, Er), spanning from blue to green shades, as represented in the color coordinates (Figure 4, right).

In summary, this work reports a ultrafast, cheap, and easily scalable microwave route to prepare pure hexagonal NaYF₄:Yb,Ln³⁺ nanorods of small size with strong upconversion luminescence. The process allows an easy coating with hydrophilic or hydrophobic molecules to render the rods dispersible in solvents of different nature. The crystal growth process is kinetically controlled by the short reaction time and permits the choice of multiple active ions (Er, Tm, Tb, etc.) without strongly affecting the nanorods crystallinity, morphology, or size. Thus tunable visible colors can be readily prepared by rational selection of the doping ions. Owing to their small size, excellent crystallinity, and good dispersibility, these nanorods could be used for a wide range of application.. Therefore, it is expected that this simple and ultrafast route to prepare the so-used NaYF₄ nanocrystals will be warmly

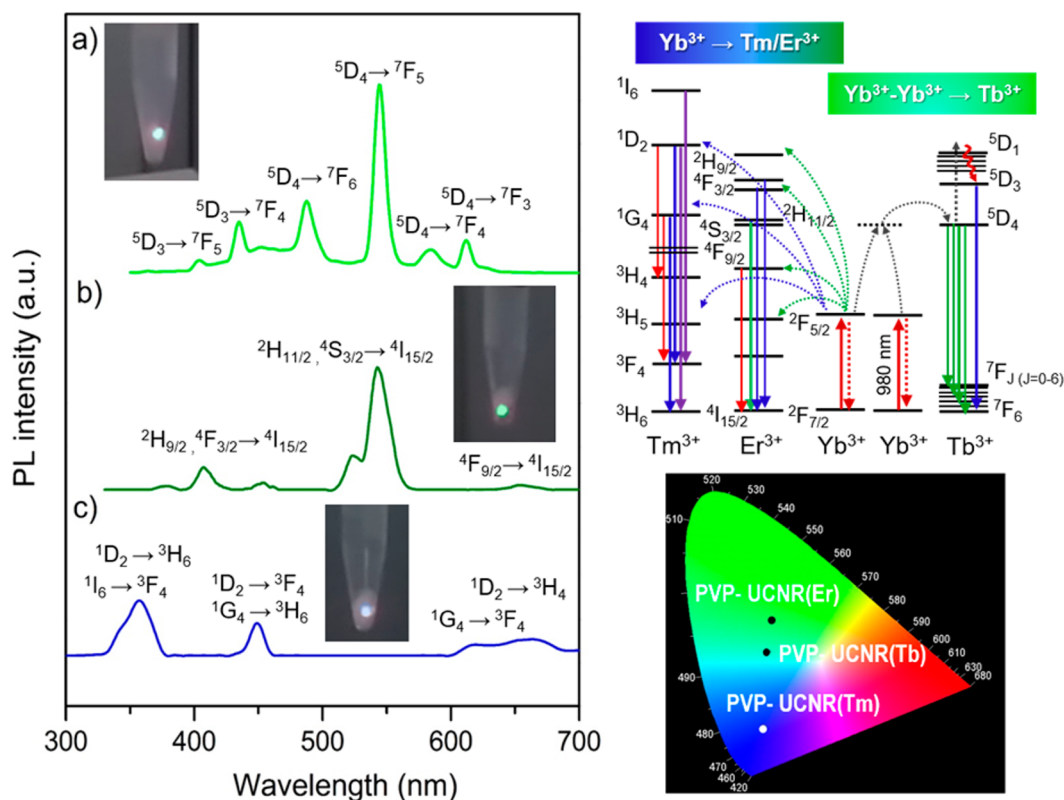


Figure 4. Left: Images of the emission in powdered samples and relative UC emission spectra for water suspensions of (a) PVP-UCNR(Tb), (b) PVP-UCNR(Er), and (c) PVP-UCNR(Tm) under 980 nm diode laser excitation. Right: Proposed energy-transfer mechanisms in the Yb:NaYF₄ nanorods codoped with Tm³⁺, Er³⁺, and Tb³⁺. The full arrows represent photon excitation and emission processes, while dotted and dashed arrows represent energy transfer and multiphonon relaxation processes, respectively. Corresponding CIE chromaticity coordinates of the UCNRs.

received by the big research community working on up-conversion nanomaterials.

■ ASSOCIATED CONTENT

Supporting Information

The Supporting Information is available free of charge on the ACS Publications website at DOI: 10.1021/acs.jpcllett.7b02473.

Synthesis reactants, microwave-assisted synthetic route, surface coating, characterization techniques used, details of synthesis variations (including XRD results and TEM micrographs), as well as FTIR characterization of the UCNs. (PDF)

■ AUTHOR INFORMATION

Corresponding Authors

*E-mail: julian@uji.es (B.J.-L.).

*E-mail: roig@icmab.es (A.R.).

ORCID

Fabrizio Guzzetta: 0000-0003-2253-8947

Anna Roig: 0000-0001-6464-7573

Beatriz Julián-López: 0000-0003-1019-776X

Notes

The authors declare no competing financial interest.

■ ACKNOWLEDGMENTS

This research was partially funded by the Spanish Ministry of Economy (MAT2015-64442-R, MAT2015-64139-C4-1-R, and SEV-2015-0496 projects, cofunded with European Social Funds) and Universitat Jaume I (PIB2014-21). F.G. thanks Generalitat Valenciana for his Grisolia Ph.D. Fellowship. We thank Olatz Arriga, nanoscience and nanotechnology student at the UAB, for her assistance in sample processing.

■ REFERENCES

- (1) Nadort, A.; Zhao, J. B.; Goldys, E. M. Lanthanide upconversion luminescence at the nanoscale: fundamentals and optical properties. *Nanoscale* **2016**, *8*, 13099–13130.
- (2) Zhou, J.; Liu, Q.; Feng, W.; Sun, Y.; Li, F. Upconversion luminescent materials: advances and applications. *Chem. Rev.* **2015**, *115*, 395–465.
- (3) Zhou, B.; Shi, B.; Jin, D.; Liu, X. Controlling upconversion nanocrystals for emerging applications. *Nat. Nanotechnol.* **2015**, *10*, 924–936.
- (4) Yi, G. S.; Chow, G. M. Synthesis of hexagonal-phase NaYF₄:Yb,Er and NaYF₄:Yb,Tm nanocrystals with efficient up-conversion fluorescence. *Adv. Funct. Mater.* **2006**, *16*, 2324–2329.
- (5) Boyer, J. C.; Vetrone, F.; Cuccia, L. A.; Capobianco, J. A. Synthesis of colloidal upconverting NaYF₄ nanocrystals doped with Er³⁺, Yb³⁺ and Tm³⁺, Yb³⁺ via thermal decomposition of lanthanide trifluoroacetate precursors. *J. Am. Chem. Soc.* **2006**, *128*, 7444–7445.
- (6) Li, D. D.; Shao, Q. Y.; Dong, Y.; Jiang, J. Q. A facile synthesis of small-sized and monodisperse hexagonal NaYF₄:Yb³⁺, Er³⁺ nanocrystals. *Chem. Commun. (Cambridge, U. K.)* **2014**, *50*, 15316–15318.
- (7) Yu, S.; Gao, X.; Jing, H.; Zhao, J.; Su, H. A synthesis and up-conversion photoluminescence study of hexagonal phase NaYF₄:Yb,Er nanoparticles. *CrystEngComm* **2013**, *15*, 10100.
- (8) Heer, S.; Kompe, K.; Gudiel, H. U.; Haase, M. Highly efficient multicolour upconversion emission in transparent colloids of lanthanide-doped NaYF₄ nanocrystals. *Adv. Mater.* **2004**, *16*, 2102–2105.
- (9) Carling, C. J.; Boyer, J. C.; Branda, N. R. Remote-control photoswitching using NIR light. *J. Am. Chem. Soc.* **2009**, *131*, 10838–10839.
- (10) Wang, L. Y.; Li, Y. D. Na(Y_{1.5}Na_{0.5})F₆ single-crystal nanorods as multicolor luminescent materials. *Nano Lett.* **2006**, *6*, 1645–1649.
- (11) Wang, Y. H.; Cai, R. X.; Liu, Z. H. Controlled synthesis of NaYF₄:Yb,Er nanocrystals with upconversion fluorescence via a facile hydrothermal procedure in aqueous solution. *CrystEngComm* **2011**, *13*, 1772–1774.
- (12) Mai, H. X.; Zhang, Y. W.; Si, R.; Yan, Z. G.; Sun, L. D.; You, L. P.; Yan, C. H. High-quality sodium rare-earth fluoride nanocrystals: Controlled synthesis and optical properties. *J. Am. Chem. Soc.* **2006**, *128*, 6426–6436.
- (13) Baghbanzadeh, M.; Carbone, L.; Cozzoli, P. D.; Kappe, C. O. Microwave-assisted synthesis of colloidal inorganic nanocrystals. *Angew. Chem., Int. Ed.* **2011**, *50*, 11312–11359.
- (14) Yu, S. M.; Hachtel, J. A.; Chisholm, M. F.; Pantelides, S. T.; Laromaine, A.; Roig, A. Magnetic gold nanotriangles by microwave-assisted polyol synthesis. *Nanoscale* **2015**, *7*, 14039–14046.
- (15) Goetz, J.; Nonat, A.; Diallo, A.; Sy, M.; Sera, I.; Lecointre, A.; Lefevre, C.; Chan, C. F.; Wong, K. L.; Charbonniere, L. J. Ultrabright lanthanide nanoparticles. *ChemPlusChem* **2016**, *81*, 526–534.
- (16) Li, F. F.; Li, C. G.; Liu, X. M.; Chen, Y.; Bai, T. Y.; Wang, L.; Shi, Z.; Feng, S. H. Hydrophilic, upconverting, multicolor, lanthanide-doped NaGdF₄ nanocrystals as potential multifunctional bioprobes. *Chem. - Eur. J.* **2012**, *18*, 11641–11646.
- (17) Niu, N.; He, F.; Gai, S.; Li, C.; Zhang, X.; Huang, S.; Yang, P. Rapid microwave reflux process for the synthesis of pure hexagonal NaYF₄:Yb³⁺,Ln³⁺,Bi³⁺ (Ln³⁺ = Er³⁺, Tm³⁺, Ho³⁺) and its enhanced UC luminescence. *J. Mater. Chem.* **2012**, *22*, 21613–21623.
- (18) Wang, H. Q.; Nann, T. Monodisperse upconverting nanocrystals by microwave-assisted synthesis. *ACS Nano* **2009**, *3*, 3804–3808.
- (19) Li, F.; Li, C.; Liu, J.; Liu, X.; Zhao, L.; Bai, T.; Yuan, Q.; Kong, X.; Han, Y.; Shi, Z.; Feng, S. Aqueous phase synthesis of upconversion nanocrystals through layer-by-layer epitaxial growth for in vivo X-ray computed tomography. *Nanoscale* **2013**, *5*, 6950–6959.
- (20) Ullah, S.; Hazra, C.; Ferreira-Neto, E. P.; Silva, T. C.; Rodrigues-Filho, U. P.; Ribeiro, S. J. L. Microwave-assisted synthesis of NaYF₄:Yb³⁺/Tm³⁺ upconversion particles with tailored morphology and phase for the design of UV/NIR-active NaYF₄:Yb³⁺/Tm³⁺@TiO₂ core@shell photocatalysts. *CrystEngComm* **2017**, *19*, 3465–3475.
- (21) Mi, C.; Tian, Z.; Cao, C.; Wang, Z.; Mao, C.; Xu, S. Novel microwave-assisted solvothermal synthesis of NaYF₄:Yb,Er upconversion nanoparticles and their application in cancer cell imaging. *Langmuir* **2011**, *27*, 14632–14637.
- (22) Som, S.; Das, S.; Yang, C. Y.; Lu, C. H. Enhanced upconversion of NaYF₄:Er³⁺/Yb³⁺ phosphors prepared via the rapid microwave-assisted hydrothermal route at low temperature: phase and morphology control. *Opt. Lett.* **2016**, *41*, 464–467.
- (23) Wawrzynczyk, D.; Piatkowski, D.; Mackowski, S.; Samoc, M.; Nyk, M. Microwave-assisted synthesis and single particle spectroscopy of infrared down-and visible up-conversion in Er³⁺ and Yb³⁺ co-doped fluoride nanowires. *J. Mater. Chem. C* **2015**, *3*, 5332–5338.
- (24) Pascu, O.; Carenza, E.; Gich, M.; Estrade, S.; Peiro, F.; Herranz, G.; Roig, A. Surface reactivity of iron oxide nanoparticles by microwave-assisted synthesis; Comparison with the thermal decomposition route. *J. Phys. Chem. C* **2012**, *116*, 15108–15116.
- (25) Su, Q. Q.; Feng, W.; Yang, D. P.; Li, F. Y. Resonance energy transfer in upconversion nanoplateforms for selective biodetection. *Acc. Chem. Res.* **2017**, *50*, 32–40.
- (26) Chen, X.; Xu, W.; Zhang, L. H.; Bai, X.; Cui, S. B.; Zhou, D. L.; Yin, Z.; Song, H. W.; Kim, D. H. Large upconversion enhancement in the "islands" Au-Ag Alloy/NaYF₄:Yb³⁺, Tm³⁺/Er³⁺ composite films, and fingerprint identification. *Adv. Funct. Mater.* **2015**, *25*, 5462–5471.
- (27) Fischer, S.; Frohlich, B.; Steinkemper, H.; Kramer, K. W.; Goldschmidt, J. C. Absolute upconversion quantum yield of beta-NaYF₄ doped with Er³⁺ and external quantum efficiency of upconverter solar cell devices under broad-band excitation considering spectral mismatch corrections. *Sol. Energy Mater. Sol. Cells* **2014**, *122*, 197–207.

- (28) Wang, F.; Deng, R. R.; Wang, J.; Wang, Q. X.; Han, Y.; Zhu, H. M.; Chen, X. Y.; Liu, X. G. Tuning upconversion through energy migration in core-shell nanoparticles. *Nat. Mater.* **2011**, *10*, 968–973.
- (29) Salley, G. M.; Valiente, R.; Guedel, H. U. Luminescence upconversion mechanisms in Yb^{3+} - Tb^{3+} systems. *J. Lumin.* **2001**, *94*, 305–309.
- (30) Chen, D.; Yu, Y.; Huang, P.; Weng, F.; Lin, H.; Wang, Y. Optical spectroscopy of Eu^{3+} and Tb^{3+} doped glass ceramics containing LiYbF_4 nanocrystals. *Appl. Phys. Lett.* **2009**, *94*, 041909.
- (31) Wei, Y.; Liu, X.; Chi, X.; Wei, R.; Guo, H. Intense upconversion in novel transparent $\text{NaLuF}_4:\text{Tb}^{3+}$, Yb^{3+} glass-ceramics. *J. Alloys Compd.* **2013**, *578*, 385–388.
- (32) Gao, Y.; Hu, Y.; Ren, P.; Zhou, D.; Qiu, J. Phase transformation and enhancement of luminescence in the Tb^{3+} - Yb^{3+} co-doped oxyfluoride glass ceramics containing NaYF_4 nanocrystals. *J. Eur. Ceram. Soc.* **2016**, *36*, 2825–2830.
- (33) Dong, H.; Sun, L. D.; Wang, Y. F.; Xiao, J. W.; Tu, D. T.; Chen, X. Y.; Yan, C. H. Photon upconversion in Yb^{3+} - Tb^{3+} and Yb^{3+} - Eu^{3+} activated core/shell nanoparticles with dual-band excitation. *J. Mater. Chem. C* **2016**, *4*, 4186–4192.
- (34) Liang, H.; Chen, G.; Li, L.; Liu, Y.; Qin, F.; Zhang, Z. Upconversion luminescence in $\text{Yb}^{3+}/\text{Tb}^{3+}$ -codoped monodisperse NaYF_4 nanocrystals. *Opt. Commun.* **2009**, *282*, 3028–3031.
- (35) Bilecka, I.; Djerdj, I.; Niederberger, M. One-minute synthesis of crystalline binary and ternary metal oxide nanoparticles. *Chem. Commun. (Cambridge, U. K.)* **2008**, 886–888.
- (36) Ludi, B.; Olliges-Stadler, I.; Rossell, M. D.; Niederberger, M. Extension of the benzyl alcohol route to metal sulfides: 'non-hydrolytic' thio sol-gel synthesis of ZnS and SnS_2 . *Chem. Commun. (Cambridge, U. K.)* **2011**, *47*, 5280–5282.
- (37) Wang, M.; Liu, J.-L.; Zhang, Y.-X.; Hou, W.; Wu, X.-L.; Xu, S.-K. Two-phase solvothermal synthesis of rare-earth doped NaYF_4 upconversion fluorescent nanocrystals. *Mater. Lett.* **2009**, *63*, 325–327.
- (38) May, P. B.; Suter, J. D.; May, P. S.; Berry, M. T. The dynamics of nanoparticle growth and phase change during synthesis of β - NaYF_4 . *J. Phys. Chem. C* **2016**, *120*, 9482–9489.
- (39) Wang, M.; Dykstra, T. E.; Lou, X.; Salvador, M. R.; Scholes, G. D.; Winnik, M. A. Colloidal CdSe nanocrystals passivated by a dye-labeled multidentate polymer: Quantitative analysis by size-exclusion chromatography. *Angew. Chem., Int. Ed.* **2006**, *45*, 2221–2224.
- (40) Wang, M.; Oh, J. K.; Dykstra, T. E.; Lou, X.; Scholes, G. D.; Winnik, M. A. Surface modification of CdSe and CdSe/ZnS semiconductor nanocrystals with Poly(N,N -dimethylaminoethyl methacrylate). *Macromolecules* **2006**, *39*, 3664–3672.
- (41) Wang, M.; Felorzabih, N.; Guerin, G.; Haley, J. C.; Scholes, G. D.; Winnik, M. A. Water-soluble CdSe quantum dots passivated by a multidentate diblock copolymer. *Macromolecules* **2007**, *40*, 6377–6384.
- (42) Gargas, D. J.; Chan, E. M.; Ostrowski, A. D.; Aloni, S.; Altoe, M. V. P.; Barnard, E. S.; Sani, B.; Urban, J. J.; Milliron, D. J.; Cohen, B. E.; Schuck, P. J. Engineering bright sub-10-nm upconverting nanocrystals for single-molecule imaging. *Nat. Nanotechnol.* **2014**, *9*, 300–305.
- (43) Xue, X.; Uechi, S.; Tiwari, R. N.; Duan, Z.; Liao, M.; Yoshimura, M.; Suzuki, T.; Ohishi, Y. Size-dependent upconversion luminescence and quenching mechanism of $\text{LiYF}_4:\text{Er}^{3+}/\text{Yb}^{3+}$ nanocrystals with oleate ligand adsorbed. *Opt. Mater. Express* **2013**, *3*, 989–999.
- (44) Wang, F.; Han, Y.; Lim, C. S.; Lu, Y. H.; Wang, J.; Xu, J.; Chen, H. Y.; Zhang, C.; Hong, M. H.; Liu, X. G. Simultaneous phase and size control of upconversion nanocrystals through lanthanide doping. *Nature* **2010**, *463*, 1061–1065.
- (45) Haase, M.; Schafer, H. Upconverting Nanoparticles. *Angew. Chem., Int. Ed.* **2011**, *50*, 5808–5829.